Unsharp Masking Sharpening Detection via Overshoot Artifacts Analysis

Gang Cao, Yao Zhao, *Member, IEEE*, Rongrong Ni, *Member, IEEE*, and Alex C. Kot, *Fellow, IEEE*

***Abstract*—In this letter, we propose a new method in detecting unsharp masking (USM) sharpening operation in digital images. Overshoot artifacts are found to occur around side-planar edges in the sharpened images. Such artifacts, measured by a sharpening detector, can serve as a rather unique feature for identifying the previous performance of sharpening operation. Test results on photograph images with regard to various sharpening operators show the effectiveness of our proposed method.**

***Index Terms*—Digital forensics, image sharpening, overshoot artifacts, unsharp masking.**

I. Introduction

As digital techniques advance, substantive powerful media editing softwares make image manipulation easy and more frequent. The claimed authenticity and history of digital images can no longer be taken for granted. In order to verify the integrity and recover the processing history, it is necessary to detect the image manipulation passively.

Previous works on digital image alteration detection can be classified into two categories. In the first category, the aberrations found in scene geometric [1] and imaging pipeline [2], [3] are employed to detect the image forgeries. The statistic based approaches are also proposed in terms of image quality metrics [4] and noise characteristics [5]. Such techniques could detect whether an original photograph has been manipulated or not, but they fail to determine how an image has been altered or to identify the use of specific image altering operations [6].

In the second category, the manipulation-specific methods are designed by detecting the feature unique to each specific type of tampering operation such as contrast enhancement [6], compression [7], resampling [8] and median filtering [9]. These methods not only can determine the originality of a photo by collaborative work, but also can identify the specific tampering performed in order to recover the image processing history by individual tests.

In this letter, we focus on the blind detection of digital image sharpening manipulation, which is commonly applied as a retouching tool. While the sharpening alters the perceptual quality without changing the content of a digital image, its detection is still forensically significant. Since the sharpening may be used as the last step to hide an image forgery, its detection can serve as a warning sign for possible image forgery.

Unsharp masking (USM) [10]–[14] is the widely used sharpening method in popular softwares such as Adobe Photoshop. We mainly address here the digital image USM sharpening detection problem. The basic principle of the USM is to add a weighted highpass-filtered version back onto the signal itself. As a result, the acutance of the edges in sharpened images becomes higher. In our prior work [15], the histogram aberration feature has been proposed to detect image sharpening, but it fails to process the images with narrow pixel value histogram. Although the ringing artifacts have been considered, the strict constraints on the occurrence position and the sparsity of step edges make the successful rate of sharpening detection low. To deal with such deficiencies, such constraints are relaxed and the overshoot artifacts, a more convenient feature, are found to be incurred by the USM sharpening. The positive/negative overshoot manifests itself as an increased/decreased jump at the side-planar edges. We formally investigate the generation of such artifacts and design an efficient measure of them to serve as the feature for a thresholding classifier.

The remainder of this letter is organized as follows. In Section II, we provide a formal analysis of the overshoot artifacts. Section III briefly presents the sharpening detection algorithm, followed by the experimental results in various test scenarios in Section IV. We draw the conclusions in Section V.

II. Overshoot Artifacts Analysis

In this section, we investigate the overshoot artifacts which are generated by applying the USM sharpening operation on digital images.

A. Transition Signal Model

Considering a 1-D signal pattern $t(n)$, referred as the *ideal transition signal* in this letter:

$$t(n) = \begin{cases} C, & n = -M_l, -M_l+1, \ldots, -1 \\ C - n\tan(\alpha), & n = 0, 1, \ldots, M_r \end{cases} \quad (1)$$

where M_l and M_r are the unit length from the origin towards the left and right, respectively. C is the planar side's amplitude and

Manuscript received April 25, 2011; revised July 23, 2011; accepted July 26, 2011. Date of publication August 15, 2011; date of current version August 25, 2011. This work was supported in part by the 973 Program (2011CB302204), the National Science Foundation of China for Distinguished Young Scholars (61025013), Sino-Singapore JRP (2010DFA11010), National NSF of China (61073159) and the Fundamental Research Funds for the Central Universities (2009JBZ006). The associate editor coordinating the review of this manuscript and approving it for publication was Dr. Athanassios Skodras.

G. Cao, Y. Zhao, and R. Ni are with the Institute of Information Science, Beijing Jiaotong University, Beijing, China, and also with the Beijing Key Laboratory of Advanced Information Science and Network Technology, Beijing 100044, China (e-mail: 06112056@bjtu.edu.cn; yzhao@bjtu.edu.cn; rrni@bjtu.edu.cn).

A. C. Kot is with the School of Electrical and Electronic Engineering, Nanyang Technological University, Singapore (e-mail: eackot@ntu.edu.sg).

Color versions of one or more of the figures in this paper are available online at http://ieeexplore.ieee.org.

Digital Object Identifier 10.1109/LSP.2011.2164791

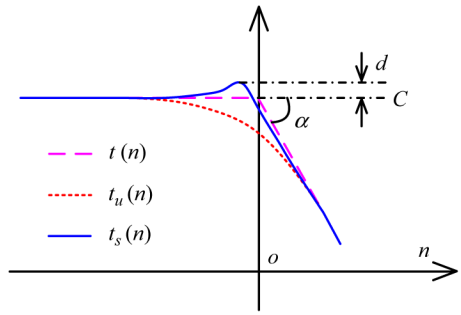

Fig. 1. Signal model of the overshoot artifacts. Here, $t(n)$, $t_u(n)$ and $t_s(n)$ denote the ideal, unsharpened and sharpened transition signal, respectively.

α is the inclination angle of the ramp signal on the other side, as shown in Fig. 1. The ideal transition signal is prepared to model the side-planar edge, which has at least one planar side, in the camera captured digital images.

When light rays go through a digital camera imaging system in the form of the ideal or slightly blurred transition signal, the edges will become more blurred to some extent, attributing to the lowpass filtering impact caused by the optical lens, limited CCD sensor resolution and color filter array interpolation. As a result, the *unsharpened transition signal* $t_u(n)$ in an unaltered image becomes smooth and can be modeled by convolving $t(n)$ and normalized Gaussian lowpass filter (GLPF) $g(n,\sigma)$ to yield

$$t_u(n) = t(n) * g(n,\sigma) \tag{2}$$

where σ is the standard deviation.

If the camera-captured image is subsequently manipulated by the USM sharpening [10]–[14], the corresponding *sharpened transition signal* $t_s(n)$ can be written as

$$t_s(n) = t_u(n) + \lambda \cdot (t_u(n) - t_u(n) * g(n,\sigma_s)) \tag{3}$$

where λ is the sharpening strength factor and σ_s is the standard deviation of the involved GLPF. Here, the sharpening operation can be described by a sharpening filter:

$$h(n,\sigma_s,\lambda) = (1+\lambda)\cdot\delta(n) - \lambda \cdot g(n,\sigma_s) \tag{4}$$

where $\delta(n)$ denotes the unit impulse function. Such sharpening filter contains negative coefficients. The value of the filtered output signal will be an affine combination of the input values, and may fall outside of the maximum/minimum value of the input signal, resulting in a positive/negative overshoot which manifests itself as an increased/decreased jump around the side-planar edges. Such overshoot is desirable in digital image sharpening due to increasing the perceived sharpness.

B. Measure of Overshoot Artifacts

To detect the overshoot artifacts, we define

$$d(t^*) = \max_{n\le 0}(t^*) - C \tag{5}$$

for $t^* = t_u, t_s$ as the measure of the overshoot.

When $t^* = t_u$, $d(t_u) \equiv 0$. It implies that the transition signal from an unsharpened image has none overshoot artifacts.

When $t^* = t_s$, it indicates that the transition signal is from a sharpened image. By letting $\nabla d(t_s) = 0$, we get the maximum value $\max_{n\le 0}(t_s) = t_s(n^*)$ at $n = n^*$, which satisfies

$$\begin{cases} \sum_{k=-\infty}^{n^*} g\left(k, \sqrt{\sigma^2+\sigma_s^2}\right) \Big/ \sum_{k=-\infty}^{n^*} g(k,\sigma) = \frac{1+\lambda}{\lambda} \\ n^* < 0 \end{cases}. \tag{6}$$

Combining (3), (5), and (6) yields

$$d(t_s) = tg(\alpha)\left((1+\lambda)\sum_{k=-\infty}^{n^*} k\cdot g(k,\sigma) - \lambda \times \sum_{k=-\infty}^{n^*} k\cdot g\left(k,\sqrt{\sigma^2+\sigma_s^2}\right)\right) \tag{7}$$

where $d(t_s)$ depends on four parameters: α, λ, σ and σ_s.

By combining (6) and (7), we get (8), shown at the bottom of the page. It can be shown after a few steps that $d(t_s) > 0$, which verifies that the USM sharpening definitively incurs the overshoot on the transition signal. The overshoot strength can be measured by $d(t^*)$ in (5). Similarly, the negative overshoot can also be detected and measured.

III. Proposed Sharpening Detection Algorithm

In the previous section, we see that the overshoot artifacts measure defined in (5) can be used as a feature to identify the sharpening operations. Given a digital image, we design the sharpening forensic detection algorithm below.

Edge Detection: Canny detector is used to get the single-pixel width edge map. Coordinates of the edge points are denoted by $\Phi_1 = \{(r_i,c_i)|i = 1,2,\ldots,N_1\}$. For color images, the detection can be applied on the luminance channel. To avoid the noise disturbance, smoothing can be applied before edge detection.

Locate Side-Planar Edges: At each edge point, we extract the corresponding crosswise pixel sequence which centers at an edge pixel and is vertical to the located edge direction. An illustration of the crosswise pixel sequence is shown in Fig. 2, where y is the pixel intensity. The pixels within $[-\omega_2-\omega_1, -\omega_1]$ and $[\omega_1, \omega_1+\omega_2]$ are used to compute the statistic (μ_l, σ_l) and

$$d(t_s) = \frac{\sum_{k_1=k_2+1}^{n^*}\sum_{k_2=-\infty}^{n^*}\left[(k_2-k_1)\cdot\left(g\left(k_1,\sqrt{\sigma^2+\sigma_s^2}\right)\cdot g(k_2,\sigma) - g\left(k_2,\sqrt{\sigma^2+\sigma_s^2}\right)\cdot g(k_1,\sigma)\right)\right]}{\sum_{k=-\infty}^{n^*} g\left(k,\sqrt{\sigma^2+\sigma_s^2}\right) - \sum_{k=-\infty}^{n^*} g(k,\sigma)}. \tag{8}$$

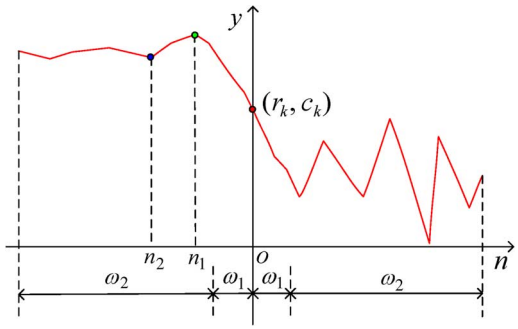

Fig. 2. The crosswise pixel sequence centered at the edge point (r_k, c_k).

(μ_r, σ_r), respectively. The side-planar edge points can then be located according to the constrains below:

$$\begin{cases} |\mu_l - \mu_r| > \tau_\mu \\ \sigma_l < \tau_\sigma \text{ or } \sigma_r < \tau_\sigma \end{cases} \tag{9}$$

where τ_μ and τ_σ are the predefined experimental thresholds. The set of side-planar crosswise pixel sequences is recorded by $\Phi_2 = \{(r_i, c_i, s) | i = 1, 2, \ldots, N_2\}$, where $s = l$ and $s = r$ denote the left and right side-planar segments, respectively. N_2 is the total number of the single planar-side cases.

Overshoot Detection: For each side-planar pixel sequence, we search the first and second polarity-changed position along the direction from center towards the planar side. For example in Fig. 2, the position n_1 and n_2 are located by polarity tracking. Let $y_i(n)$ be such a crosswise pixel sequence, where $i = 1, 2, \ldots, N_2$ and $n \in [-\omega_2 - \omega_1, \omega_1 + \omega_2]$. Compute

$$d_i = \max_{n \in [n_2, n_1]} \{y_i(n)\} - \max_{n \in [-\omega_1 - \omega_2, n_2]} \{y_i(n)\}. \tag{10}$$

The overshoot is judged as present if $d_i > \tau_d$, and the overshoot strength can be measured by d_i. The set of side-planar crosswise pixel sequences in which the overshoot has been detected is marked by $\Phi_3 = \{(r_i, c_i, s) | i = 1, 2, \ldots, N_3\}$. Here, N_3 is the total number of the overshoot-detected single planar-side cases.

Overshoot Metric: The overshoot metric for the global image is defined below as the average strength of all overshoot points in Φ_3. That is,

$$f = \frac{1}{N_3} \sum_{i=1}^{N_3} d_i. \tag{11}$$

Such a metric is used in a thresholding classifier to identify the image sharpening operation. The test image is considered as sharpened if $f > \tau_o$, where τ_o denotes the threshold used by the classifier.

The proposed sharpening detection process can be summarized in the following steps.

Step 1) Detect image edges using Canny detector.
Step 2) Locate the side-planar edges according to (9).
Step 3) Detect and measure the overshoot artifacts via (11).
Step 4) Apply thresholding to detect the USM sharpening.

IV. Experimental Results and Discussion

In order to evaluate the proposed sharpening detection algorithm, we collect 400 photograph images which are captured by several cameras in different lighting conditions and saved in JPEG format with the size from 1200 × 900 to 2832 × 2128 pixels. The content of these images consist of various natural scenes. The green channel of each image is used to create the unaltered image set. For simulating the practical scenarios, we prepare various sizes of unsharpened images including the original size and its scaled versions with height $\mathrm{H} = 1000$ and 500 pixels via aspect ratio invariant. Such unsharpened images are processed by different USM sharpening algorithms to create the corresponding sharpened image set.

For evaluating the performance of the sharpening detection technique, each test image is classified by determining if it is sharpened or not using a series of decision thresholds. Experimentally, we set $\omega_1 = 1$, $\omega_2 = 6$, $\tau_\mu = 100$, $\tau_\sigma = 10$, $\tau_d = 11$. Such setting can be easily adjusted within a limited range without affecting the detection results. The probabilities of detection $(\mathrm{P_d})$ and false alarm $(\mathrm{P_{fa}})$ determined by thresholds are calculated as the percentage of the sharpened images correctly classified and that of the unsharpened images incorrectly classified, respectively. The receiver operating characteristic (ROC) curves are generated for evaluation.

Test results on different size of image sets are shown in Fig. 3(a). Here, the sharpening is implemented by Gaussian lowpass filtering mask method [10] with $\sigma_s = 1$ and $\lambda = 1$. At $\mathrm{P_{fa}} = 10\%$, $\mathrm{Pd} = 95\%$ for $\mathrm{H} = 500$. As expected, the detection performance on the smaller size images is better than that on the larger size images due to the lowpass filtering effect of downsampling, which impairs the image acutance and the overshoot artifacts. Comparing to the prior method in [15], the proposed algorithm achieves higher detection rates, especially in the case of lower $\mathrm{P_{fa}}$ and larger image sizes.

To test the detection performance under different sharpening strengths, different settings of σ_s and λ are used to simulate the sharpening. In what follows, the image set with $\mathrm{H} = 1000$ pixels is used for testifying. Fig. 3(b) shows that the higher detection rate can be obtained when the stronger sharpening is applied.

Results for assessing the robustness of our proposed algorithm are reported in Fig. 3(c). It indicates that the sharpening detection method is robust against post-JPEG compression and additional Gaussian white noise (AGWN). Even for the low quality JPEG compression $(\mathrm{Q} = 40)$ and intense noise $(\sigma = 3)$, the sharpening operation can still be detected.

To investigate the generalization capability of the sharpening detector, six USM sharpening algorithms are implemented for testing. Besides the commonly used Gaussian and Laplace mask methods [10], the nonlinear category such as Quadratic and Cubic operators [11], the adaptive category such as local statistic based [12] and recursive update based [13] are also tested. Results in Fig. 4(a) verify the efficacy of the detector. The detection rates for all sharpening methods achieve above 88% when $\mathrm{P_{fa}} = 10\%$. It should be noted that our technique is limited to the USM-like sharpening which produces overshoot.

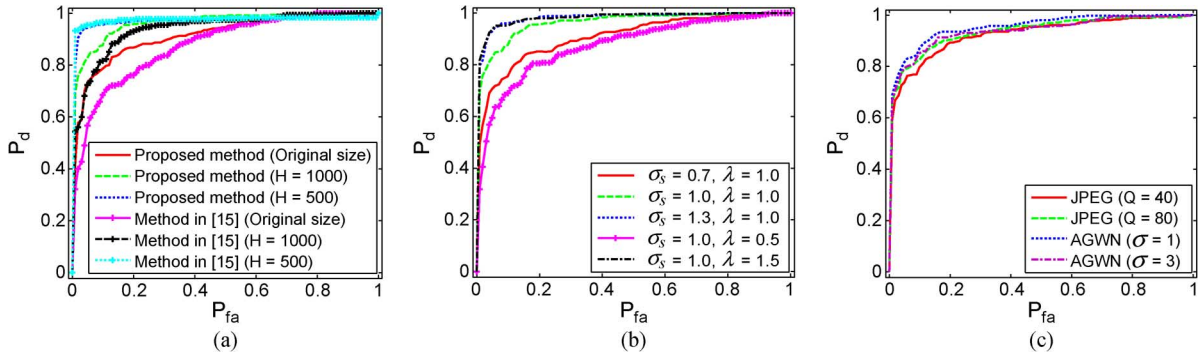

Fig. 3. Sharpening detection ROC curves (a) for images with different sizes; (b) for different sharpening strengths; (c) under different postprocessing.

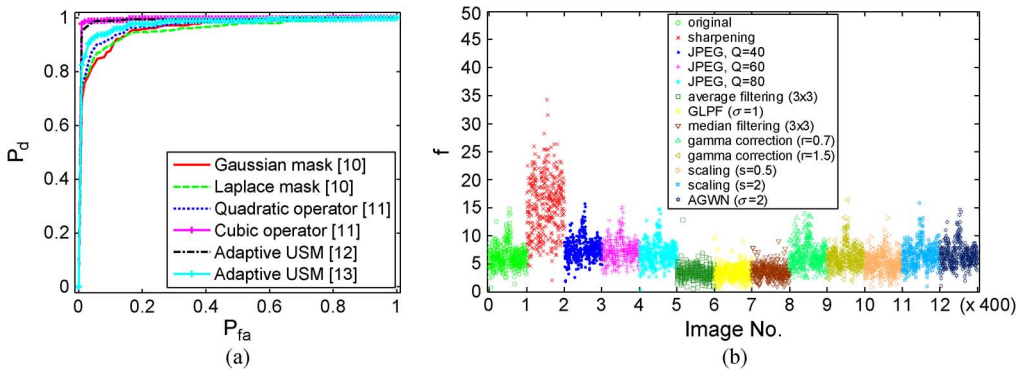

Fig. 4. (a) Sharpening detection ROC curves under different sharpening algorithms. (b) Feature value distribution for different manipulations.

Recall that the primary objective of the sharpening forensic detection is to find a unique feature caused by sharpening but not by other manipulations. Are the overshoot artifacts unique to the USM sharpening? A simple but effective verification is to observe the feature value distribution of the sample images operated by different manipulations. Feature values of the sample images processed by each type of operation are displayed in Fig. 4(b). We can see that the feature values of the sharpened images are higher than those of others, and can be differentiated by thresholding. From such an intuitive comparison, we can observe that the overshoot artifacts could be considered as a dominating feature of the USM sharpening operations.

V. Conclusions

As an image forensics problem, we propose a technique to detect USM sharpening. We detect and measure the overshoot artifacts occurred around side-planar edges as a good feature in sharpening identification. Experimental results show that our proposed algorithm works extremely well for small size images undergone USM sharpening operation. The detector is verified to be robust against post-JPEG compression and noising. Such a sharpening detection algorithm may be extended to detect the image splicing forgery with different sharpening histories.

References

[1] M. K. Johnson and H. Farid, "Exposing digital forgeries in complex lighting environments," *IEEE Trans. Inf. Forensics Secur.*, vol. 2, no. 3, pp. 450–461, 2007.

[2] M. Chen, J. Fridrich, M. Goljan, and J. Lukáš, "Determining image origin and integrity using sensor noise," *IEEE Trans. Inf. Forensics Secur.*, vol. 3, no. 1, pp. 74–90, Mar. 2008.

[3] A. C. Popescu and H. Farid, "Exposing digital forgeries in color filter array interpolated images," *IEEE Trans. Signal Process.*, vol. 53, no. 10, pp. 3948–3959, Oct. 2005.

[4] S. Bayram, I. Avcubas, B. Sankur, and N. Memon, "Image manipulation detection," *J. Electron. Imag.*, vol. 15, no. 4, pp. 04110201–04110217, 2006.

[5] H. Gou, A. Swaminathan, and M. Wu, "Noise features for image tampering detection and steganalysis," in *Proc. IEEE Int. Conf. on Image Processing*, San Antonio, 2007, pp. VI-97–VI-100.

[6] M. C. Stamm and K. J. R. Liu, "Forensic detection of image manipulation using statistical intrinsic fingerprints," *IEEE Trans. Inf. Forensics Secur.*, vol. 5, no. 3, pp. 492–506, 2010.

[7] W. Luo, J. Huang, and G. Qiu, "JPEG error analysis and its applications to digital image forensics," *IEEE Trans. Inf. Forensics Secur.*, vol. 5, no. 3, pp. 480–491, 2010.

[8] A. C. Popescu and H. Farid, "Exposing digital forgeries by detecting traces of resampling," *IEEE Trans. Signal Process.*, vol. 53, no. 2, pp. 758–767, 2005.

[9] G. Cao, Y. Zhao, R. Ni, L. Yu, and H. Tian, "Forensic detection of median filtering in digital images," in *Proc. Int. Conf. on Multimedia and Expo*, Singapore, 2010, pp. 89–94.

[10] R. C. Gonzalez and R. E. Woods, *Digital Image Processing (2nd Edition)*. Upper Saddle River, NJ: Prentice-Hall, 2002.

[11] G. Ramponi, N. Strobel, S. K. Mitra, and T.-H. Yu, "Nonlinear unsharp masking methods for image contrast enhancement," *J. Electron. Imag.*, vol. 5, no. 3, pp. 353–366, 1996.

[12] J. S. Lee, "Digital image enhancement and noise filtering by using local statistics," *IEEE Trans. Patt. Anal. Mach. Intell.*, vol. PAMI-2, pp. 165–168, 1980.

[13] A. Polesel, G. Ramponi, and V. J. Mathews, "Image enhancement via adaptive unsharp masking," *IEEE Trans. Image Process.*, vol. 9, no. 3, pp. 505–510, 2000.

[14] G. de Haan, *Digital Video Post Processing*. Eindhoven, The Netherlands: Univ. Eindhoven Press, 2010.

[15] G. Cao, Y. Zhao, and R. Ni, "Detection of image sharpening based on histogram aberration and ringing artifacts," in *Proc. IEEE Int. Conf. on Multimedia and Expo*, New York, 2009, pp. 1026–1029.